International Journal of Engineering & Technology, 7 (3.27) (2018) 601-608

International Journal of Engineering & Technology

Website: www.sciencepubco.com/index.php/IJET

Research paper



Texture Classification based on First Order Circular and Elliptical Ternary Direction Pattern Matrix

K. Subba Reddy[1], V. Vijaya Kumar[2], A.P. Siva Kumar[3]

[1]Research Scholar, Jawaharlal Nehru Technological University, Anantapur, Ananthapuramu, Andhra Pradesh, India.
Associate Professor, Department of Computer Science and Engineering , Rajeev Gandhi Memorial college of Engineering and Technology, Nandyal, Andhra Pradesh, India.
[2]Director- Rayalaseema University, Kurnool, India
[3]Professor, Department of Computer Science and Engineering, Jawaharlal Nehru Technological University, Ananthapuramu, Andhra Pradesh, India.
**Corresponding author E-mail: mrsubbareddy@yahoo.com , drvvk114@gmail.com , sivakumar.ap@gmail.com*

Abstract

Local binary pattern (LBP) captures isotropic structural information and completely fails in representing anisotropic information, however the horizontal elliptical LBP (H-ELBP) and vertical elliptical LBP (V-ELBP) represents partial anisotropic information only. In our earlier work we have derived "circular and elliptical-LBP (CE-LBP)" captures both isotropic and anisotropic structural information with a feature vector size equivalent to LBP and it is easy to implement and invariant to monotonic illumination changes. The LBP, local ternary pattern (LTP), CE-LBP and most of the extensions of LBP descriptor basically ignore the directional information. To address this and to capture both isotropic and anisotropic directional information, this paper proposes a "circular and elliptical ternary direction pattern matrix (CE-TDPM)". The CE-TDPM encodes the relationship between the central pixel and two of its neighboring pixel located in different angles (α, β) with different directions. The CE-TDPM evaluated the possible direction variation pattern for central pixel by measuring the first order derivate relationship among the horizontal and vertical neighbors (0° vs. 90°; 90° vs. 180°; 180° vs. 270°; 270° vs. 0°) and derived a unique code. The performance of the proposed method is compared with various other existing methods using the benchmark texture databases viz. Brodtaz, UIUC, Outex and MIT-VisTex. The performance analysis shows the efficiency of the proposed method over the existing methods.

Keywords: *Isotropic; Anisotropic; Derivative; Ternary pattern*

1. Introduction

TEXTURE is one of the most important visual patterns and it represents the spatial arrangement of intensities of pixels of an image. Decent representation of texture is most important, crucial and beneficial in various applications like in video indexing [1], Content based image retrieval (CBIR) [2], lip reading [3], multi-resolution representation to deal with scale changes [4], sound-event classification [5], texture segmentation [6], web search [7] texture classification [8-10], scene recognition [11], object detection [12, 13] and image matching [14]. Illumination variation is a major issue in texture representation and it should be eliminated. The illumination may vary over different blocks of an image i.e. shadows and non-shadows. Illumination variation tends to be more or less uniform in local regions and they can be dealt efficiently by applying local neighborhood based methods. That's why local based methods have become more popular in image classification when compared to global based methods. Further illumination variation in a local neighborhood can be viewed as monotonic gray-level changes. The illumination variations in local neighborhoods can be dealt effectively by finding the intensity differences between pixels instead of intensities of each and every individual pixel. In fact in the literature the texture spectrum [15] and the local binary pattern [8, 16] approaches computes the intensity differences between center and neighboring pixels of a neighborhood. These methods have become popular in dealing with illumination variations. The aim of any texture representation scheme is to derive significant features that are robust to the variations of pose, viewpoint changes illumination, rotation and scale. There are many large extrinsic variations and complex intrinsic structures present in natural textures and that's why the texture classification has become a challenging problem to derive a robust classification approach [17, 20]. Various feature descriptors have been proposed over the past decades.

Texton-based methods are popular and succeeded in the texture analysis in the early years. The texton based methods initially derived filter banks by dividing the image into 2 x 2 blocks and based on the filter bank responses texture patterns are derived [21, 22]. Later many methods based on local neighborhood responses are proposed in the literature and the noted ones are scale-invariant feature transform (SIFT) [23], Histogram of oriented gradients (HOG) [24], local binary patterns (LBP) [8] and its extensions [25- 32]. The local features derived by these methods can be easily integrated with other complex methods [33] like gray level co-occurrence matrix (GLCM) [34, 35] and these integrated methods could able to detect local structures, edges, orientation and other salient features. Some of the complicated and advanced methods are proposed in the literature: histogram model known as weber local descriptor (WLD) [36], to match the original image regions a patch model [37], to detect environmental changes in a

Copyright © 2018 Authors. This is an open access article distributed under the Creative Commons Attribution License, which permits unrestricted use, distribution, and reproduction in any medium, provided the original work is properly cited.

robust manner a wavelet-based multi-fractal spectrum (WMFS)[38] model, to represent the local regions with curves from gradients oriented texture curves (OTC) [39] model, improved local difference binary (ILDB) [40] model. The high-level features with semantic information can be obtained by deep learning methods easily. The deep learning techniques and deep learning features are studied recently in texture classification [41-46]. However mostly many researchers treated the texture representation as a low level problem.

After finding the significant features recently many advanced classification methods, are investigated for classification purpose which include multinomial logistic regression [47, 48], support vector machines (SVMs) [49, 50], random forest [51], neural network [52], rotation forest [53] and sparse representation-based classifier (SRC) [54-57]. The SRC is different from previous classifiers which make decisions based on standard classifiers (e.g., k-nearest-neighbor [58] or SVMs [49], the decision rule of SRC is based on the minimum reconstruction error and it is used in many applications SRC [59-66]. All the above LBP based approaches and its extensions derived features from circular neighborhood. These methods have not considered any other topology and these methods basically have not considered the derivative directions. To address this, present paper extracts local features on optimized circular, horizontal and vertical elliptical neighborhood named as circular and elliptical neighborhood (CEN) and derives ternary derivative direction pattern code that captures both circular and elliptical derivative information.

The rest of this paper is organized as follows. The proposed method presented in Section 2. In Section 3, results, discussions and comparisons with other methods is carried out under various natural databases. Section 4 concludes the paper.

2. Derivation of Circular and Elliptical-Ternary Derivative Pattern Matrix (CE-TDPM)

Local binary patterns (LBP) [16] have emerged as one of the most prominent and widely studied local texture descriptors in the field of computer vision and pattern recognition. This is mainly because of the merits of LBP i.e., simplicity, ability to capture image micro-structures, and robustness to illumination variations. The LBP represents the circular topology and in the literature different kinds of topologies that represent different kinds of structural information are derived. In the literature the topologies that represent horizontal and vertical lines [67], the lines and disk in terms of local quantized pattern (LQP) [68] are explored on LBP to have more discrimination power. Shu Liao et al. [69] derived Elliptical local binary patterns (ELBP) to exploit elliptical topology and later they are expanded to derive parabolic, hyperbolic, and spiral neighborhood topologies [70] and the local patterns and the local code on these i.e. elliptical, parabolic and hyperbolic, are derived in the same way as LBP.

The circular neighborhood of LBP, represents only isotropic structural information and whereas the ELBP derives only anisotropic structural information. The LBP completely oversights the anisotropic information and the ELBP on the other hand completely fail in recognizing the isotropic information. To address this in our earlier work we have proposed circular and elliptical LBP (CE-LBP)[71],which represents more powerful isotropic and anisotropic information of the local neighborhood.

The common problem of LBP based methods like LBP, LTP, CE-LBP etc., is all of them pay no attention to the spatial distribution characteristics of texture in images e.g., the varying texture features in different directions. This will cause some loss of important and functional texture information and by which the classification performance will be degraded. The texture information is derived using grey level variations between centre and neighboring pixel in two directions only i.e. positive or negative in LBP based methods. And they completely ignore the information regarding the direction of local features. This observation made us to propose the computation of gray-level derivative variation patterns on different directions and construct the spatial distribution pattern.

The grey level value of a pixel represents the fundamental information of a texture image. The difference between adjacent neighboring pixels also represents useful information and however it lacks the participation of central pixel, therefore it will miss the significant and fundamental information. To address this, the present paper initially derives first order derivatives between centre pixel and sampling points of circular and elliptical neighborhood (CEN).The block diagram of the proposed model is given in Figure 1.

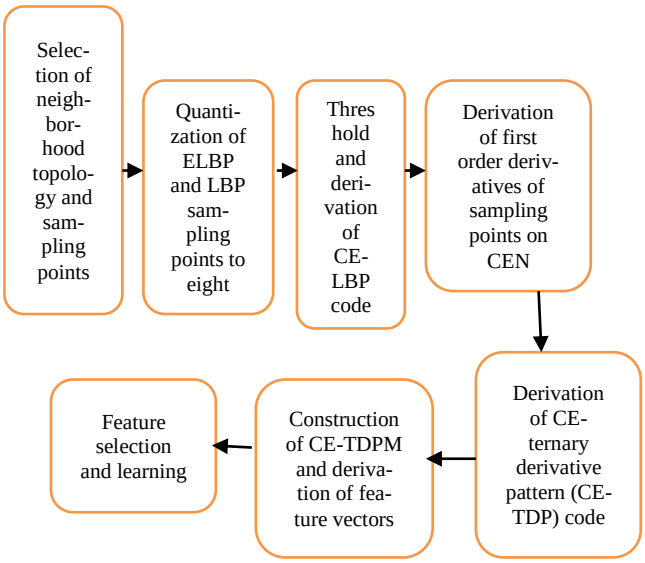

Figure 1: The block diagram of the proposed CE-TDPM.

2.1 The Derivation of LBP

The basic LBP represents a circular neighborhood with radius R=1 and with 8-neighboring pixels i.e. a 3 x 3 neighborhood and this was later extended to higher radius "R" with different number of sampling or neighboring pixels. The computer vision and image processing domains like age classification, face recognition, medical image processing and texture classification requires both isotropic and anisotropic features for high success rate. However to derive complete anisotropic information one should consider both Horizontal and Vertical Elliptical structures and this creates lot of complexity. To have complete isotropic and anisotropic topology one should consider LBP, which represents complete Circular topology, Horizontal elliptical LBP representing partial elliptical topology and vertical elliptical LBP representing the other part of elliptical topology. The micro information of the texture in ELBP model is usually captured by using horizontal and vertical ELBP's. Our earlier work derived a completely new variant of LBP and ELBP, called CE-LBP, to capture both isotropic and anisotropic structural information, with minimal complexity and without losing any information from both the topologies. The basic LBP is derived on a 3 x3 neighborhood. The local patterns are derived in LBP, by thresholding the 8-neighboring pixels of 3x3 neighborhood with the value of centre pixel (Figure 2).

S_1	S_2	S_3
S_8	S_c	S_4
S_7	S_6	S_5

Figure 2: 3 x 3 basic LBP neighborhood.

The LBP considers only sign information, to derive local binary patterns of the neighborhood, because of which the LBP is invariant to monotonic illumination changes. The LBP code of a pixel (x_c,y_c) is defined as :

$$LBP_{d,R}(x_c,y_c) = \sum_{i=1}^{n} S(S_i - S_c) * 2^{i-1}$$

$$\text{where } S(x) = \begin{cases} 1, & x \geq 0 \\ 0, & x < 0 \end{cases} \quad (1)$$

Where Sc is the intensity value of centre pixel (x_c,y_c), Si corresponds to the intensities of S-neighboring/ sampling pixels located on a circle of radius R centered at S_c. In practice, the neighboring pixels are sampled on a circle. The LBPd,R(x_c,y_c) derives an unique decimal number ranges from 0 to 2^S-1.

2.2 The derivation of CE-LBP

To derive elliptical shape or elliptical neighboring or sampling points in both horizontal and vertical elliptical structures one need to consider horizontal (x-axis) radius, the vertical (y-axis) radius and the number of sampling points of the ellipse and they are usually denoted as 'hR' , 'vR' and 'S' respectively. The relationship between hR and vR determines the type of elliptical shape: vertical or horizontal and is given in the following algorithm. The basic representation of LBP, H-ELBP and V-ELBP is given in Figure 3.

Algorithm 1:
begin
Step 1: If hR == vR
Then given structure is circular i.e. forms a LBP
Step 2: if hR < vR
Then given structure is horizontal ellipse i.e. forms a H-ELBP
Step 3: if hR < vR
Then given structure is vertical ellipse i.e. forms a V-ELBP
end;

The neighboring pixel co-ordinates (xi, yi) of the centre pixel (x_c,y_c) in elliptical structures are derived based on the following equations.

$$\text{angle-step} = 2*\pi/n \quad (2)$$

$$x_i = x_c + hR*(\cos(i-1)*\text{angle-step}) \quad (3)$$

$$y_i = x_c + vR*(\cos(i-1)*\text{angle-step}) \quad (4)$$

The unique decimal code for $H - ELBP^{d,hR,vR}(x_c,y_c)$ and V-ELBPd,hR,vR (x_c,y_c) at each centre pixel (x_c,y_c) is derived similar to LBP based on equation 5 and 6.

$$ELBP^{d,hR,vR}(x_c,y_c) = \sum_{i=1}^{P} s\left(d_i^{n,hR,vR} - d_c\right).2^{i-1} \quad \textbf{(5)}$$

Where S(x) is defined as

$$S(x) = f(x) = \begin{cases} 1, & if x \geq 0 \\ 0, & x < 0 \end{cases} \quad \textbf{(6)}$$

The decimal codes of conventional LBP, H-ELBP and V-ELBP with 8-sampling or neighboring pixels ranges from 0 to 28-1 (255). Therefore to capture complete anisotropic information, we have to club both the histograms H-ELBP and V-ELBP i.e histogram ranges from 0 to 511. This gives a huge and huge histogram and thus increases dimensionality to a huge extent and thus not suitable for any applications.

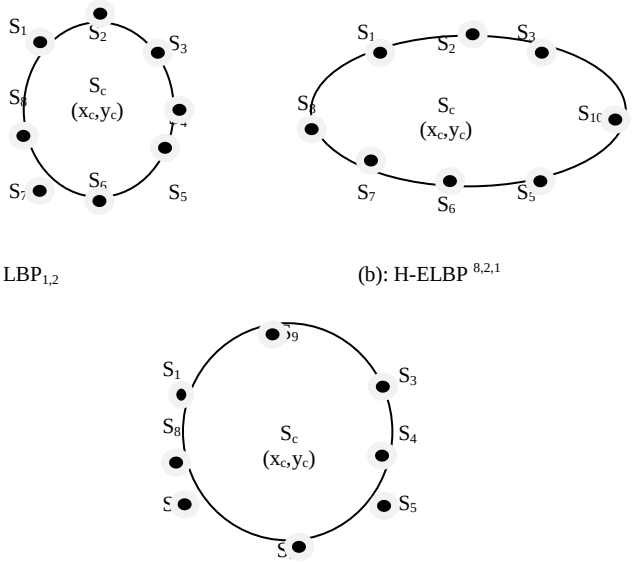

(a): $LBP_{1,2}$ (b): H-ELBP ^{8,2,1}

(c): V-ELBP ^{8,1,2}

Figure 3: The representation of basic LBP, H-ELBP and V-ELBP.

The interesting feature of the basic LBP, H-ELBP and V-ELBP is all three operators require 8-neighboring pixels around the centre pixel (x_c, y_c) i.e Sc as shown in Figure 3. Out of these, the diagonal sampling pixels S_1, S_3, S_5 and S_7 are common among the three local patterns i.e. the LBP, H-ELBP and V-ELBP (Figure 3 and Figure 4(a)). The LBP and H-ELBP have two other sampling points S_2 and S_6 as common, where as S_4 and S_8 are common sampling points in between LBP and V-LBP only (Figure 3 and Figure 4(a)). The sampling points $\{S_9, S_{11}\}$ and $\{S_{10}, S_{12}\}$ are only required for V-ELBP and H-ELBP respectively (Figure 3 and Figure 4(a)). A huge histogram of size 2^{12-1} is required, to capture both complete isotropic and anisotropic features completely, if one considers all the 12 sampling points to represent all the three descriptors, which is high in complexity and may not suits for many applications (Figure 4(a)). The above histogram range can be reduced to 0 to 767, if one concatenates the individual histograms of the three operators or descriptors.

		S_9		
	S_1	S_2	S_3	
S_{12}	S_8	S_c	S_4	S_{10}
	S_7	S_6	S_5	
		S_{11}		

(a): The sampling points of LBP and V-ELBP and H- ELBP.

S_1	$(S_2+ S_9)$	S_3
$(S_8+ S_{12})$	S_c	$(S_4+ S_{10})$
S_7	$(S_6 +S_{11})$	S_5

(b): The quantized sampling points of V-ELBP and H- ELBP. CE-LBP

Figure 4: The quantization process of sampling points of CE-LBP over the centre pixel Sc.

Our earlier work "circular and elliptical LBP (CE-LBP)" quantizes the total number of sampling points around Sc of circular and elliptical neighborhood, into 8 pixels by representing complete isotropic and anisotropic information as shown in Figure 4(b). The CE-LBP code of a pixel Sc with co-ordinate position (x_c, y_c) is derived as

$$CE - LBP_{(d,R1,R2)} = \sum_{i=1}^{8} S(S_i - S_c) * 2^{i-1} \quad (7)$$

with

$$s(x) = \begin{cases} 1, & \text{if } x \geq 0 \\ 0, & \text{if } x < 0 \end{cases} \quad (8)$$

where R1, hR and vR corresponds to the 'R' of LBP, H-ELBP and V-ELBP respectively. The R2 corresponds to 'hR' of H-ELBP and 'vR'- of V-ELBP. The CE-LBP$_{(8,1,2)}$ code ranges from 0 to 255, with complete isotropic and anisotropic information.

2.3 The Derivation of CE-TDPM

The present paper derived four first order derivatives from sampling points that forms 0°, 90°, 180° and 270° around the central pixel of the CEN and they can be represented as

$$FD - CEN_{0^o}(S_c) = 2 * f(Sc) - (f(S4) + f(S10)) \quad (9)$$

$$FD - CEN_{90^o}(S_c) = 2 * f(Sc) - (f(S2) + f(S9)) \quad (10)$$

$$FD - CEN_{180^o}(S_c) = 2 * f(Sc) - (f(S8) + f(S12)) \quad (11)$$

$$FD - CEN_{270^o}(S_c) = 2 * f(Sc) - \big(f(S6) + f(S11)\big) \quad (12)$$

In the above the FD-CEN$_0{}^0$ and FD-CEN$_{180}{}^0$ represents the sampling points that are combined between circular and horizontal elliptic neighborhood. And in the same way FD-CEN$_{180}{}^0$ and FD-CEN$_{270}{}^0$ combines vertical elliptic and circular neighborhood. This paper strongly believes that a good and high amount of texture information can be extracted between two first order grey level derivative direction sampling pixels that forms an angle □^{o} with respect to central pixel. Based on this assumption this paper derived a ternary relationship between two first order derivatives of circular and elliptical neighborhood (CEN).And these patterns are named as circular and elliptical ternary direction patterns (CE-TDP).The CE-TDP derives a strong relationship between two first order grey level direction sampling points of CEN that forms an angle of 90^0 with respect to center pixel. This paper derived CE-TDP matrix(CE-TDPM) from the CE-TDP coded image for texture classification and the block diagram of this is given in Figure 1.

The present paper derived four different CE-TDPs between two first order grey level direction sampling points of CEN located with angle of αo and βo around the central pixel. The four CE-TDP are defined between i. 0° vs. 90° (CE-TDP1(S_c)) ii. 90° vs. 180° (CE-TDP2(S_c)) iii. 180° vs. 270° (CE-TDP3(S_c)) iv. 270° vs. 0° (CE-TDP4(S_c))

$$CE - TDPi\ (S_c) = \begin{cases} 2 & FD - CEN_{\alpha^o}(S_c) \geq 0 \text{ and } FD - CEN_{\beta^o}(S_c) \geq 0 \\ 1 & FD - CEN_{\alpha^o}(S_c) < 0 \text{ and } FD - CEN_{\beta^o}(S_c) > 0 \\ & \text{or} \\ & FD - CEN_{\alpha^o}(S_c) > 0 \text{ and } FD - CEN_{\beta^o}(S_c) < 0 \\ 0 & FD - CEN_{\alpha^o}(S_c) < 0 \text{ and } FD - CEN_{\beta^o}(S_c) < 0 \end{cases} \quad (13)$$

One of the ternary patterns (0, 1, 2) will be assigned to CE-TDP by comparing the first order derivatives located at angle αo and βo with the central pixel (two local derivatives). The present paper derives a unique decimal number from these four CE-TDPs by concatenating the ternary values with base 3 as given in the Eq. 14 and this unique decimal number represent the direction of the structural pattern. This decimal number is denoted as CE-TDP code. The CE-TDP code ranges from 0 to 80.

$$CE - TDPc = \sum_{p=1}^{4} 3^{p-1} * CE - TDPp\ (S_c) \quad (14)$$

Where CE-TDPi(S_c)will have one of the three possible ternary values {0,1,2}.

This paper computed GLCM on CE-TDP coded image and derived CE-TDPM and the four GLCM features on CE-TDPM are evaluated.

1. Contrast :

$$\text{Contrast} = \sum_{n=0}^{M-1} n^2 \left\{\sum_{i=1}^{M} \sum_{j=1}^{N} X(i,j)\right\}, |i-j| = n \quad (15)$$

2. Correlation :

$$\text{Correlation} = \sum_{i=0}^{M-1} \sum_{j=0}^{N-1} \frac{\{iXj\}XX(i,j) - \{\mu_x X \mu_y\}}{\sigma_x X \sigma_y} \quad (16)$$

3. Energy :

$$\text{Energy} = \sum_{i,j} X(i,j)^2 \quad (17)$$

4. Homogeneity or Angular Second Moment (ASM):

$$\text{ASM} = \sum_{i=0}^{G-1} \sum_{j=0}^{G-1} \{X(i,j)\}^2 \quad (18)$$

3. Results and Discussions

To investigate the classification accuracy, we have identified four well known and popular texture databases i.e.Brodtaz [72], UIUC [73], Outex [74] and MIT-VisTex [75].The images of these databases are captured under varying conditions like lighting, illumination and varying sizes. Each database consists of various classes and each class consists of various images. This paper compared the proposed CE-TDPM descriptor with LBP, CE-LBP, ULBP based methods, H-ELBP, V-ELBP and concatenation of H-ELBP and, V-ELBP (HV-ELBP). This paper used the machine learning classifiers Liblinear and multilayer perceptron for classification purpose.

This paper selected 30 different homogeneous texture images from Brodtaz database with a dimension of 640 x 640 pixels. The sample images are shown in Figure 5. This paper divided each image into 25 non-overlapped texture images of size 128x128. This results a dataset of 750 images (30 x 25). The proposed classifiers were trained by using 10 samples of each class (30 x 10=300 images in total and the remaining 15 samples per class were used for validation (30 x 15=450 images in total).

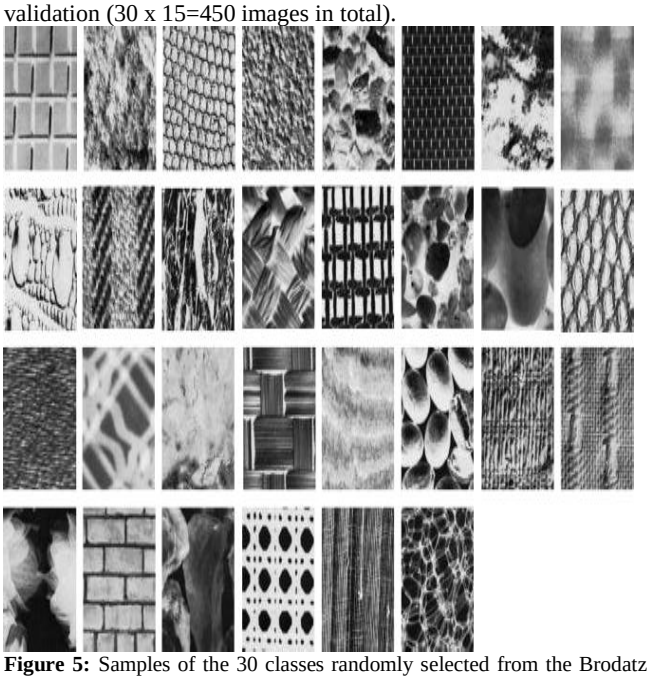

Figure 5: Samples of the 30 classes randomly selected from the Brodatz database.

The sample images of UIUC database are shown in Figure 6. This database includes 25 classes and each class consists of 40 images. This results a total of 1000(25x40) texture images. The size of each image is 640x480. In our experiments we have partitioned 640 x 480 images into 15 non-overlapped images of size 128x128. This leads to a total of 15000 (25x 40 x 15) images and a total of 600 (40 x 15=600) images per class. In our texture classification experiments, 300 training images are randomly chosen from each class, while the remaining 300 images are used as test set.

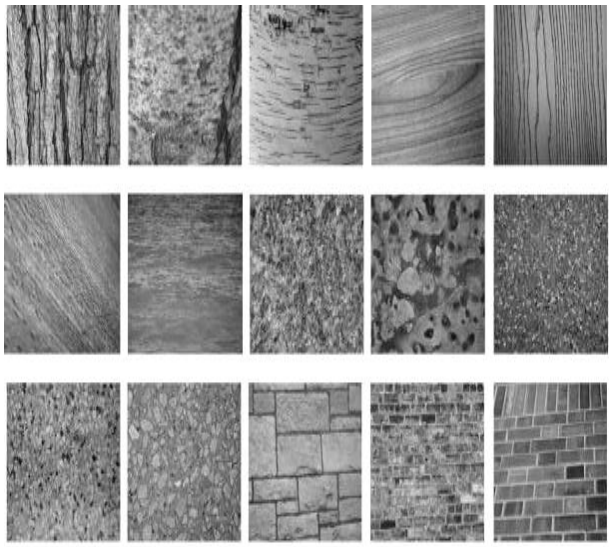

Figure 6: Samples of the 25 classes from the UIUC database.

The Outex database contains two test suits: Outex-TC-10(TC12-000) and Outex-TC-12(TC12-001). Two subsets of the Outex dataset, testsuite TC10 (also known as Outex_TC_00010 in [74]) and testsuite TC12 (also known as Outex_TC_00012 in [74]) are used for texture classification. Both TC10 and TC12 are composed of 24 texture classes of images under 128 × 128 resolutions for nine rotation angles (0°, 5°, 10°, 15°, 30°, 45°, 60°, 75°,and 90°) and on each rotation angle, there are 20 images. These images are captured under three illumination conditions namely 1. "inca' 2. t184 3. Horizon. The total number of images in TC10 and TC12 are 4320 and 9120, respectively. All images in TC10 are under the same illuminant inca, and this leads to 4320 (24 × 9 × 20 = 4320) images in total. , There are 480 images in TC12 under inca in a single direction (24 x 20=480). There are 4320 t184 images and 4320 horizon images in TC12 under nine rotation angles (24 x 20 x 9=4320). This leads to a total of 9120 images in TC12. Both TC10 and TC12 share the same training dataset of the 480 "inca" images but use different test datasets.

For the TC10 dataset, with illumination condition "inca" with 0o of rotation (24 x 20=480 images), is used for training purpose in the present paper. The remaning images with other 8-rotations are used for testing (24 x 8 x 20=3840 images). For TC-12 dataset, the 24 x 20 images of illumination "inca" and rotation angle zero degrees are adopted for the training process. All the 24 x 20 x9 samples captured under illumination (tl84 or horizon) are used as test data for TC12 dataset. The sample images from Outex database are shown in Figure 7.

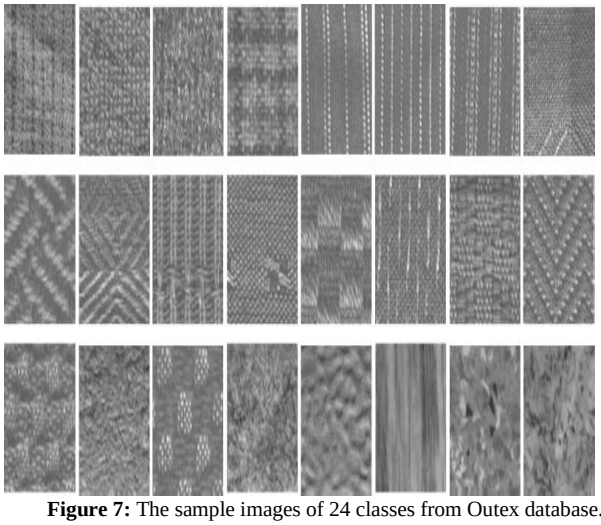

Figure 7: The sample images of 24 classes from Outex database.

MIT- VisTex database is taken that contains 40 textures [75]. Every texture has a size of 512X512 being categorizes into sixteen 128X128 non-overlapped sub-images and therefore, designed 640 (40X16) images database. The sample images are shown in Figure 8.



Figure 8: The sample textures from MIT-VisTex texture database.

The texture classification results of the proposed CE-TDPM is compared with existing methods and listed in Table 1,2 , 3 and 4 for Brodtaz[72], UIUC[73], Outex[74] and MIT-VisTex [75] databases respectively. The following are noted down.

From Table 1 i.e. the classification results on the Brodtaz textures, the following findings are noted down. The proposed CE-TDPM outperformed the LBP, H-ELBP, V-ELBP and concatenation of horizontal and vertical ELBP models. The basic reason for this, the CE-TDPM captures the both isotropic and anisotropic structure information. The LBP with complete isotropic structural model attained an average of 3% high classification rate than the partial anisotropic models: H-ELBP or V-ELBP. The process of concatenating the H-ELBP and V-ELBP increased the dimensionality twice when compared to LBP and it attained almost similar classification rate of LBP. The proposed CE-TDPM attained high classification rate of over LBP, partial anisotropic structures (H-ELBP and V-ELBP) and complete anisotropic structure HV-ELBP respectively. The ULBP and concatenation of Horizontal and Vertical EULBP (HV-EULBP) attained almost same classification rate, however the feature vector size is doubled in the case of HV-EULBP descriptor.

The experimental results on various variants of LBP on UIUC dataset using various classifiers are placed in Table 2 and the proposed CE-TDPM attained a better classification rate on all three classifiers on UIUC dataset, when compared to LBP and ELBP descriptors.

The Table 3 displays the experimental results on the Outex dataset and the partial anisotropic models: H-ELBP or V-ELBP exhibited a low performance of 1% when compared to LBP. The HV-ELBP has shown slightly high classification rate than LBP model. The proposed CE-TDPM attained high classification rate when compared to all other descriptors.

Table 1: Classification rate on Brodtaz dataset.

S.No	Name of the method	Liblinear	Multilayer Perceptron	Average
1	LBP	90.02	91.82	90.92
2	H-ELBP	89.48	90.01	89.75
3	V-ELBP	88.28	89.24	88.76
4	H U V-ELBP	90.24	90.84	90.54
5	ULBP	86.20	87.25	86.73
6	H-ULBP	85.44	84.23	84.84
7	V-ULBP	86.32	85.27	85.80
8	HUV –ULBP	87.21	87.28	87.25
9	CE-ULBP	92.48	93.25	92.87
10	CE-LBP	93.72	94.68	94.20
11	Proposed CE-TDPM	94.02	96.07	95.04

Table 2: Classification rate on UIUC dataset.

S.No	Name of the method	Liblinear	Multilayer Perceptron	Average
1	LBP	54.65	56.27	55.46
2	H-ELBP	52.25	53.89	53.07
3	V-ELBP	53.08	54.25	53.67
4	H U V-ELBP	54.08	55.96	55.02
5	ULBP	52.28	53.18	52.73
6	H-ULBP	49.97	52.16	51.07
7	V-ULBP	48.67	50.12	49.40
8	HUV –ULBP	53.67	55.27	54.47
9	CE-ULBP	57.21	60.02	58.62
10	CE-LBP	60.72	62.88	61.80
11	Proposed CE-TDPM	65.78	71.52	68.65

Table 3: Classification rate on Outex dataset.

		TC-10		TC-12 ’t’		TC-12 ‘h’	
S.No	Name of the method	LL	MLP	LL	MLP	LL	MLP
1	LBP	84.87	85.52	65.19	66.32	64.03	65.63
2	H-ELBP	83.45	84.68	64.18	65.36	63.23	64.58
3	V-ELBP	84.02	85.67	63.76	64.85	63.06	64.85
4	HV-ELBP	85.05	86.36	64.28	65.98	64.48	65.39
5	ULBP	79.98	81.21	61.90	62.38	60.01	61.35
6	H-ULBP	80.24	81.86	59.82	60.35	58.84	59.68
7	V-ULBP	81.03	82.34	58.74	59.68	58.91	59.48
8	HUV – ULBP	81.76	82.65	60.91	61.48	60.25	61.35
9	CE-ULBP	87.84	88.91	70.94	71.63	70.21	72.15
10	CE-LBP	90.24	91.28	73.89	74.68	72.91	73.68
11	Proposed CE-TDPM	93.87	95.09	79.28	81.25	76.56	77.67

Table 4: Classification rate on MIT-VisTex dataset.

S.No	Name of the method	Liblinear	Multilayer Perceptron	Average
1	LBP	56.36	63.68	60.02
2	H-ELBP	59.65	66.36	63.01
3	V-ELBP	60.52	59.63	60.08
4	H U V-ELBP	63.12	65.36	64.24
5	ULBP	56.69	60.53	58.61
6	H-ULBP	50.36	53.32	51.84
7	V-ULBP	53.63	56.63	55.13
8	HUV –ULBP	56.62	62.32	59.47
9	CE-ULBP	61.23	68.62	64.93
10	CE-LBP	69.68	70.32	70.00
11	Proposed CE-TDPM	71.36	75.69	73.53

The multilayer perceptron on all databases by using proposed and existing methods have shown high performance than liblinear classifier. The graph of Figure 9 and 10 display the average classification rate of the proposed method and existing methods (Figure 9 only LBP based methods and Figure 10 only uniform local pattern based methods)using multilayer perceptron. The graph of Figure 9 and 10 clearly indicates the proposed CE-TDPM outperforms the existing methods on each database.

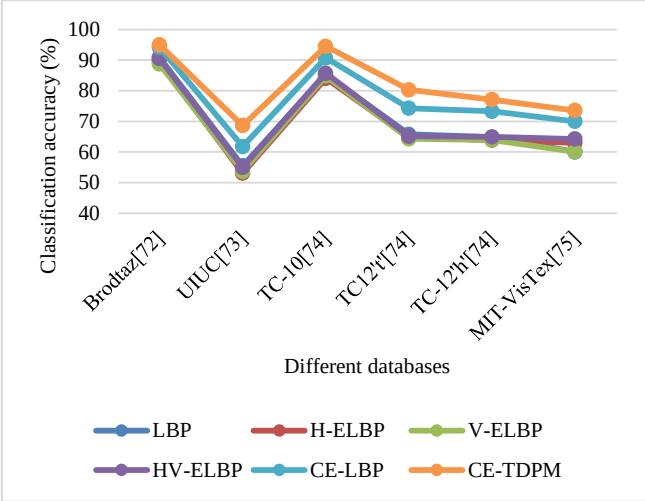

Figure 9: Average classification graph database wise on LBP based methods.

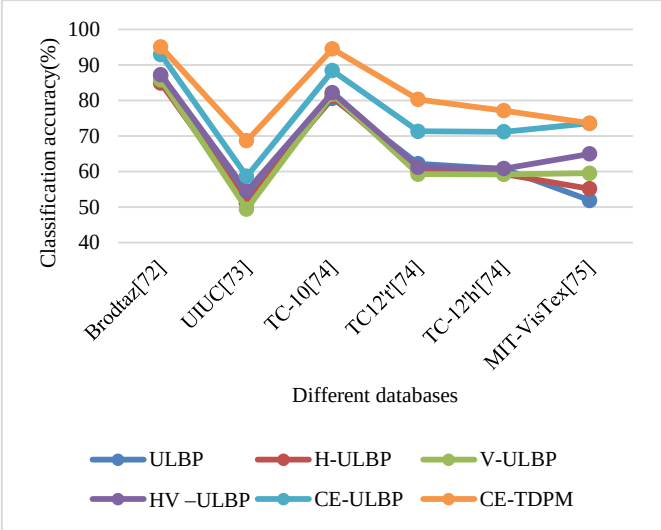

Figure 10: ULBP based average classification graph on different databases.

The following Table 5 gives the dimension of the existing and the proposed descriptors, with the type of information they capture. From the table it is evident that the proposed CE-TDPM captures both isotropic and anisotropic ternary direction patterns with a low dimensionality.

Table 5: Description about the dimensions of proposed and existing descriptors.

S.No		Name of the descriptor	Dimension	Type of information	
				Isotropic	Anisotropic
1	Existing methods	$LBP_{8,1}$	256	Yes	No
2		$H\text{-}ELBP_{8,2,1}$	256	No	Yes (Partial)
3		$V\text{-}ELBP_{8,1,2}$	256	No	Yes (Partial)
4		$H\text{-}ELBP_{8,2,1}$ U $V\text{-}ELBP_{8,1,2}$	512	No	Yes(total)
5		$LBP_{(8,1)}$ U $UH\text{-}ELBP_{(8,2,1)}$ U $V\text{-}ELBP_{(8,1,2)}$	768	Yes	Yes
6		$CE\text{-}LBP_{(8,1,2)}$	256	Yes (total)	Yes (total)
7		CE-	58	Yes (total)	Yes (total)

		$ULBP_{(8,1,2)}$			
8	Proposed method	CE-TDPM	80	Yes With derivative direction information	Yes With derivative direction information

4. Conclusions

The present paper derived a new variant to LBP, elliptical LBP and CE-LBP by exploring disadvantages of LBP and LBP-like methods and found that they have ignored completely the direction responses around the central pixel. The proposed CE-TDPM descriptor captures both isotropic and anisotropic structural information without increasing any dimension. The CE-TDPM holds more powerful information in terms of ternary derivative patterns that are derived with an angle with respect to central pixel of CEN. The CE-TDPM used first order horizontal and vertical pixels relationship with central pixel of CEN and derived a ternary direction pattern. The performance of the proposed method is compared with the LBP, LTP, LBPv, TS and CDTM methods. The range of CE-TDPM greatly reduced to 0 to 80 when compared to 0 to 255 (in case of LBP, CE-LBP, H-ELBP, V-ELBP) and 0 to 3561 (in case of LTP). The GLCM on CE-TDPM will have a dimension of 80 x 80 and it also reduced the dimensionality of GLCM from 255 x 255 in case of LBP, CE-LBP, H-ELBP, V-ELBP and LTP based methods. The extensive experimental results on the referred data bases clearly demonstrate the efficacy of the proposed descriptor over the existing ones.

References

[1] M. Haas, J. Rijsdam, B. Thomee, and M. S. Lew, "Relevance feedback: Perceptual learning and retrieval in bio-computing, photos, and video", in Proc. 6th ACM SIGMM Int. Workshop Multimedia Inf. Retrieval, 2004, pp. 151–156.

[2] X.-Y.Wang, B.-B. Zhang, and H.-Y. Yang, "Content-based image retrieval by integrating color and texture features", Multimedia Tools Appl., vol. 68, no. 3, pp. 545–569, 2014

[3] G. Zhao, M. Barnard, and M. Pietikainen, "Lipreading with local spatiotemporal descriptors", IEEE Trans.Multimedia, vol. 11, no. 7, pp. 1254– 1265, Nov. 2009.

[4] Y. D. Chun, N. C. Kim, and I. H. Jang, "Content-based image retrieval Using multiresolution color and texture features", IEEE Trans.Multimedia, vol. 10, no. 6, pp. 1073–1084, Oct. 2008.

[5] J. Ren, X. Jiang, J. Yuan, and N. Magnenat-Thalmann, "Sound-event classification using robust texture features for robot hearing", IEEE Trans. Multimedia, vol. 19, no. 3, pp. 447–458, Mar. 2017

[6] X. Liu and D.Wang, "Image and texture segmentation using local spectral histograms", IEEE Trans. Image Process., vol. 15, no. 10, pp. 3066–3077,Oct. 2006.

[7] X. Wang, C. Zhang, and Z. Zhang, "Boosted multi-task learning for face verification with applications to web image and video search", in Proc. IEEE Conf. Comput. Vision Pattern Recognit., 2009, pp. 142–149.

[8] T. Ojala, M. Pietik¨ainen, and T. M¨aenp¨a¨a, "Multiresolution gray-scale and rotation invariant texture classification with local binary patterns", IEEE Trans. Pattern Anal. Mach. Intell., vol. 24, no. 7, pp. 971–987, Jul. 2002.

[9] T. Song, H. Li, F. Meng, Q. Wu, and B. Luo, "Exploring space-frequency co-occurrences via local quantized patterns for texture representation", Pattern Recogit., vol. 48, no. 8, pp. 2621–2632, 2015.

[10] Y. Dong, J. Feng, L. Liang, L. Zheng, and Q. Wu, "Multiscale samplingbased texture image classification", IEEE Signal Process. Lett., vol. 24,no. 5, pp. 614–618, May 2017.

[11] T. Song and H. Li, "WaveLBP based hierarchical features for image classification", Pattern Recognit. Lett., vol. 34, no. 12, pp. 1323–1328, 2013.

[12] D. T. Nguyen, Z. Zong, P. Ogunbona, and W. Li, "Object detection using non-redundant local binary patterns", in Pro. 17th Int. Conf. Image Process., Sep. 2010, pp. 4609–4612.

A. Satpathy, X. Jiang, andH. L. Eng, "LBP-based edge-texture features for object recognition", IEEE Trans. Image Process., vol. 23, no. 5, pp. 1953– 1964, May 2014.

[13] M. Heikkil¨a, M. Pietik¨ainen, and C. Schmid, "Description of interestregions with local binary patterns", Pattern Recognit., vol. 42, no. 3,pp. 425–436, 2009.

[14] LiWangDong-ChenHe, "Texture classification using texture spectrum", Pattern Recognition Volume 23, Issue 8, 1990, Pages 905-910.

[15] T. Ojala, M. Pietik¨ainen, and D. Harwood, "A comparative study of texture measures with classification based on featured distributions", Pattern Recognit., vol. 29, no. 1, pp. 51–59, 1996.

[16] U.Kandaswamy, S. A. Schuckers, and D. Adjeroh, "Comparison of texture analysis schemes under nonideal conditions", IEEE Trans. Image Process., vol. 20, no. 8, pp. 2260–2275, Aug. 2011

[17] G. S. Xia, G. Liu, X. Bai, and L. Zhang, "Texture characterization usingshape co-occurrence patterns", IEEE Trans. Image Process., vol. 26,no. 10, pp. 5005–5018, Oct. 2017.

[18] F. Juefei-Xu and M. Savvides, "Subspace-based discrete transform encoded local binary patterns representations for robust periocular matching on NIST's face recognition grand challenge", IEEE Trans. Image Process., vol. 23, no. 8, pp. 3490–3505, Aug. 2014.

[19] T. Song, H. Li, F. Meng, Q. Wu, and J. Cai, "LETRIST: Locally encoded transform feature histogram for rotation-invariant texture classification", IEEE Trans. Circuits Syst. Video Technol., to be published.

[20] O. G. Cula and K. J. Dana, "Compact representation of bidirectional texture functions", in Proc. IEEE Conf. Comput. Vision Pattern Recognit., 2001, vol. 1, pp. I-1041–I-1047.

[21] T. Leung and J. Malik, "Representing and recognizing the visual appearance of materials using three-dimensional textons", Int. J. Comput. Vision, vol. 43, no. 1, pp. 29–44, 2001.

[22] D. G. Lowe, "Distinctive image features from scale-invariant keypoints",Int. J. Comput. Vision, vol. 60, no. 2, pp. 91–110, 2004.

[23] N. Dalal and B. Triggs, "Histograms of oriented gradients for humandetection", in Proc. IEEE Conf. Comput. Vision Pattern Recognit., 2005,vol. 1, pp. 886–893.

[24] X. Meng, Z. Wang, and L. Wu, "Building global image features for scenerecognition", Pattern Recognit., vol. 45, no. 1, pp. 373–380, 2012.

[25] X. Tan and B. Triggs, "Enhanced local texture feature sets for face recognition under difficult lighting conditions", IEEE Trans. Image Process., vol. 19, no. 6, pp. 1635–1650, Jun. 2010.

[26] Y. Guo, G. Zhao, and M. Pietik¨ainen, "Texture classification using a linear configuration model based descriptor", in Proc. Brit. Mach. Vision Conf., Pietik¨a, pp. 1–10.

[27] G. Sharma, S. ulHussain, and F. Jurie, "Local higher-order statistics (LHS) for texture categorization and facial analysis", in Proc. Eur. Conf. Comput. Vision, 2012, pp. 1–12.

[28] L. Wolf, T. Hassner, and Y. Taigman, "Descriptor based methods in the wild", in Proc. Workshop Faces in "Real-Life" Images: Detection, Alignment, Recognit., 2008, pp. 1–14.

[29] Z. Guo, L. Zhang, and D. Zhang, "A completed modeling of local binarypattern operator for texture classification", IEEE Trans. Image Process.,vol. 19, no. 6, pp. 1657–1663, Jun. 2010.

[30] X. Wu and J. Sun, "Joint-scale LBP: A new feature descriptor for texture classification", Vis. Comput., vol. 33, pp. 317–329, 2015.

[31] L. Liu, P. Fieguth, Y. Guo, X. Wang, and M. Pietik¨ainen, "Local binary features for texture classification: Taxonomy and experimental study", Pattern Recognit., vol. 62, pp. 135–160, 2017.

[32] N. Zhang, R. Farrell, F. Iandola, and T. Darrell, "Deformable part descriptors for fine-grained recognition and attribute prediction", in Proc. IEEE Int. Conf. Comput. Vision, 2013, pp. 729–736.

[33] B. Sujatha, V.Vijaya Kumar, P. Harini, "A new logical compact LBP co-occurrence matrix for texture analysis", International Journal of Scientific & Engineering Research (IJSER) , Vol.3, Iss.2, 2012, pp.1-5, ISSN 2229-5518.

[34] V. VijayaKumar ,Jangala. SasiKiran , V.V. HariChandana, " An effective age classification using topological features based on compressed and reduced grey level model of the facial skin", International journal of image, graphics and signal processing (IJIGSP), , Vol.6, Iss.1, 2013, pp.9-17, ISSN: 2074-9082.

[35] J. Chen et al., "WLD: A robust local image descriptor", IEEE Trans.Pattern Anal. Mach. Intell., vol. 32, no. 9, pp. 1705–1720, Sep. 2010.

[36] J. Mao, J. Zhu, and A. L. Yuille, "An active patch model for real world texture and appearance classification", in Proc. Eur. Conf. Comput. Vision, 2014, pp. 140–155.

[37] Y. Xu, X. Yang, H. Ling, and H. Ji, "A new texture descriptor using multifractal analysis in multi-orientation wavelet pyramid", in Proc. IEEE Conf. Comput. Vision Pattern Recognit., 2010, pp. 161–168.
[38] R. Margolin, L. Zelnik-Manor, and A. Tal, "OTC: A novel local descriptorfor scene classification", in Proc. Eur. Conf. Comput. Vision., 2014,pp. 377–391.
[39] T. Gao, X. Zhao, M. Xiang, and Z. Liu, "Texture feature descriptor usingauto salient feature selection for scale-adaptive improved local difference binary", Multidimensional Syst. Signal Process., vol. 28, pp. 281–292, 2017.
[40] M. Cimpoi, S. Maji, I. Kokkinos, S. Mohamed, and A. Vedaldi, "Describing textures in the wild", in Proc. IEEE Conf. Comput. Vision Pattern Recognit., 2014, pp. 3606–3613.
[41] E. Simo-Serra et al., "Discriminative learning of deep convolutionalfeature point descriptors", in Proc. IEEE Int. Conf. Comput. Vision, 2015, pp. 118–126.
[42] E. Simo-Serra et al., "Discriminative learning of deep convolutionalfeature point descriptors", in Proc. IEEE Int. Conf. Comput. Vision, 2015, pp. 118–126.
[43] M. Cimpoi, S. Maji, and A. Vedaldi, "Deep filter banks for texture recognition and segmentation", in Proc. IEEE Conf. Comput. Vision Pattern Recognit., 2015, pp. 3828–3836.
[44] L. Sifre and S. Mallat, "Rotation, scaling and deformation invariant scattering for texture discrimination", in Proc. IEEE Conf. Comput. Vision Pattern Recognit., 2013, pp. 1233–1240.
[45] T.-Y. Lin and S. Maji, "Visualizing and understanding deep texture representations", in Proc. IEEE Conf. Comput. Vision Pattern Recognit., 2016, pp. 2791–2799.
[46] V. Andrearczyk and P. F. Whelan, "Using filter banks in convolutionalneural networks for texture classification", Pattern Recognit. Lett., vol. 84, pp. 63–69, 2016.
[47] J. Li, J. M. Bioucas-Dias, and A. Plaza, "Semi-supervised hyperspectralimage classification using soft sparse multinomial logistic regression",IEEE Geosci. Remote Sens. Lett., vol. 10, no. 2, pp. 318–322, Mar. 2013.
[48] J. Li, J. M. Bioucas-Dias, and A. J. Plaza, "Spectral-spatial hyper spectral image segmentation using subspace multinomial logistic regression and Markov random fields", IEEE Trans. Geosci. Remote Sens., vol. 50, no. 3, pp. 809–823, Mar. 2012.
[49] F.Melgani and L. Bruzzone, "Classification of hyperspectral remote sensing images with support vector machines", IEEE Trans. Geosci. Remote Sens., vol. 42, no. 8, pp. 1778–1790, Aug. 2004.
[50] M. Fauvel, J. A. Benediktsson, J. Chanussot, and J. R. Sveinsson, "Spectral and spatial classification of hyperspectral data using SVMs and morphological profiles", IEEE Trans. Geosci. Remote Sens., vol. 46, no. 11, pp. 3804–3814, Nov. 2007.
[51] J. Xia, M. D. Mura, J. Chanussot, P. Du, and X. He, "Random subspace ensembles for hyperspectral image classification with extended morphological attribute profiles", IEEE Trans. Geosci. Remote Sens., vol. 53, no. 9, pp. 4768–4786, Sep. 2015.
[52] F. Ratle, G. Camps-Valls, and J.Weston, "Semisupervised neural networks for efficient hyperspectral image classification", IEEE Trans. Geosci. Remote Sens., vol. 48, no. 5, pp. 2271–2282, May 2010.
[53] J. Xia, J. Chanussot, P. Du, and X. He, "Spectral-spatial classification for hyperspectral data using rotation forests with local feature extraction and Markov random fields", IEEE Trans. Geosci. Remote Sens., vol. 53, no. 5, pp. 2532–2546, May 2015.
[54] M. Elad, Sparse and Redundant Representations—From Theory to Applications in Signal and Image Processing. New York, NY, USA: Springer, 2010.
[55] J. Mairal, M. Elad, and G. Sapiro, "Sparse representation for color image restoration", IEEE Trans. Image Process., vol. 17, no. 1, pp. 53–69, Jan. 2008.
[56] J. Wright, A. Y. Yang, A. Ganesh, S. S. Sastry, and Y. Ma, "Robust facerecognition via sparse representation", IEEE Trans. Pattern Anal. Mach. Intell., vol. 31, no. 2, pp. 210–227, Feb. 2009.
[57] M. Elad and M. Aharon, "Image denoising via sparse and redundantrepresentations over learned dictionaries", IEEE Trans. Image Process.,vol. 15, no. 12, pp. 3736–3745, Dec. 2006.
[58] R. O. Duda, P. E. Hart, and D. G. Stork, Pattern Classification. 2nd Ed.Hoboken, NJ, USA: Wiley, 2012.
[59] Y. Chen, N. M. Nasrabadi, and T. D. Tran, "Hyperspectral image classification via kernel sparse representation", IEEE Trans. Geosci. Remote Sens., vol. 51, no. 1, pp. 217–231, Jan. 2013
[60] Y. Chen, N. M. Nasrabadi, and T. D. Tran, "Hyperspectral image classification using dictionary-based sparse representation", IEEE Trans. Geosci. Remote Sens., vol. 49, no. 10, pp. 3973–3985, Oct. 2011.
[61] J. Li, H. Zhang, Y. Huang, and L. Zhang, "Hyperspectral image classification by nonlocal joint collaborative representation with a locally adaptive dictionary", IEEE Trans. Geosci. Remote Sens., vol. 52, no. 6, pp. 3707–3719, Jun. 2014.
[62] J. Li, H. Zhang, and L. Zhang, "Column-generation kernel nonlocal joint collaborative representation for hyperspectral image classification", ISPRS J. Photogramm., vol. 94, pp. 25–36, 2014.
[63] E. Zhang, X. Zhang, H. Liu, and L. Jiao, "Fast multifeature joint sparserepresentation for hyperspectral image classification", IEEE Geosci.Remote Sens. Lett., vol. 12, no. 7, pp. 1397–1401, Jul. 2015.
[64] H. Zhang, J. Li,Y.Huang, and L. Zhang, "A nonlocal weighted joint sparse representation classification method for hyperspectral imagery", IEEE J. Sel. Topics Appl. Earth Observ. Remote Sens, vol. 7, no. 6, pp. 2056–2065, Jun. 2014.
[65] W. Li, Q. Du, and M. Xiong, "Kernel collaborative representation withTikhonov regularization for hyperspectral image classification", IEEEGeosci. Remote Sens. Lett., vol. 12, no. 1, pp. 48–52, Jan. 2015.
[66] L. Gan, P. Du, J. Xia, and Y. Meng, "Kernel fused representation-basedclassifier for hyperspectral imagery", IEEE Geosci. Remote Sens. Lett.,vol. 14, no. 5, pp. 684–688, May 2017.
[67] Petpon, S. Srisuk, Face recognition with local line binary pattern, in: International Conference on Image and Graphics, 2009, pp. 533–539.
[68] S. ulHussian and B. Triggs, "Visual recognition using local quantized patterns", in *Proc. Eur. Conf. Comput. Vis.*, 2012, pp. 716–729.
[69] S. Liao, A. C. S. Chung, Face recognition by using elongated local binary patterns with average maximum distance gradient magnitude, in: Proceedings of Asian Conference on Computer Vision (ACCV), 2007, pp. 672–679
[70] L. Nanni, A. Lumini, S. Brahnam, Local binary patterns variants as texture descriptors for medical image analysis, Artif. Intell. Med. 49 (2) (2010) 117–125
[71] K. Subba Reddy, V. Vijaya Kumar, A.P. Siva Kumar, Classification of Textures Using a New Descriptor Circular and Elliptical-LBP (CE-ELBP), International Journal of Applied Engineering Research ISSN 0973-4562 Volume 12, Number 19 (2017) pp. 8844-8853
[72] P. Brodatz, Texture, 1968, "A Photographic Album for Artists and Designers" , Reinhold, New York, 1968.
[73] S. Lazebnik, C. Schmid, and J. Ponce, "A sparse texture representationusing local affine regions", IEEE Trans. Pattern Anal. Mach. Intell.,vol. 27, no. 8, pp. 1265–1278, Aug. 2005.
[74] http://www.outex.oulu.fi/index.php?page=image_database.
[75] MIT Vision and Modeling Group, Cambridge, „Vision texture", http://vismod.media.mit.edu/pub/